Purdue University
Purdue e-Pubs

International Compressor Engineering Conference | School of Mechanical Engineering

1984

Scroll Compressor Analytical Model

E. Morishita

M. Sugihara

T. Inaba

T. Nakamura

Follow this and additional works at: https://docs.lib.purdue.edu/icec

Morishita, E.; Sugihara, M.; Inaba, T.; and Nakamura, T., "Scroll Compressor Analytical Model" (1984). *International Compressor Engineering Conference.* Paper 495.
https://docs.lib.purdue.edu/icec/495

This document has been made available through Purdue e-Pubs, a service of the Purdue University Libraries. Please contact epubs@purdue.edu for additional information.
Complete proceedings may be acquired in print and on CD-ROM directly from the Ray W. Herrick Laboratories at https://engineering.purdue.edu/Herrick/Events/orderlit.html

SCROLL COMPRESSOR ANALYTICAL MODEL

Etsuo Morishita, Central Research Laboratory,
Mitsubishi Electric Corporation, Amagasaki, Hyogo, Japan

Masahiro Sugihara, Tsutomu Inaba, Toshiyuki Nakamura, Wakayama Works,
Mitsubishi Electric Corporation, Wakayama, Japan

ABSTRACT

The efficiency of the scroll compressor which employs the axial and the radial sealing techniques is competitive with that of the other rotary and the reciprocating compressors. The bearing load and the torque are smooth so that quiet operation is realized. Therefore the machine is suitable particularly for air conditioning application.

The authors have studied the scroll compressor which utilizes an involute of a circle. The displacement volume is calculated. The axial, tangential and radial pressure components are then obtained by assuming the isentropic or polytropic processes. The equations of motion are established for the orbiting scroll and the Oldham coupling. These equations are solved analytically and the motion of the orbiting scroll and the Oldham coupling is calculated. The motion of the orbiting scroll is influenced by the inertia force of the Oldham coupling, and the radial sealing force changes with a frequency twice that of the rotation. The overturning moment which acts on the orbiting scroll is estimated, and the stability condition for the orbiting scroll is clarified.

INTRODUCTION

The scroll machine was invented by Creux[1] in 1905 and is currently attracting the designers' attention because of its high efficiency and smooth operation. Application for car compressors and air conditioning is commercialized in Japan[2),3),4)] and further development is expected.

Axial and radial sealing are the most critical techniques and have been recognized from the old days. Creux[1)] referred to the tip seal (steam-tight in Reference (1)) which was pressed axially by the spring. The radial sealing techniques are also known;[5),6)] they employ the centrifugal force of the rotating parts or produce the radial component from the pressure load by a mechanism like the swing link. The idea of the scroll fluid machinery was introduced; it was equipped with axial and tangential sealing[7),8)]. The practical development of this scroll compressor was also conducted[9),10)]. The scroll compressor appeared on the market in 1981 utilizing these two sealing techniques[2)].

The authors realized that the scroll compressor has inherent advantages (good sealing, smooth operation, stillness, no valve, simple structure, low rubbing speed, etc.) and analyzed the machine theoretically. The displacement volume is obtained from the geometric character of the involute of a circle. The tangential, radial and axial pressure loads are calculated by assuming the isentropic or polytropic compression processes.

The motion of the orbiting scroll and the Oldham coupling has not been studied so far. To clarify the design conditions, the equations of motion are established for these two parts of the scroll compressor, including the friction. The equations are solved analytically and the forces acting on the orbiting scroll and the Oldham coupling are calculated. The inertia force of the Oldham coupling is transmitted to the orbiting scroll. The radial sealing force is necessarily influenced and changes with a frequency twice that of the rotation. The overturning moment which acts on the orbiting scroll is estimated, and the stability condition is given for the orbiting scroll.

GEOMETRIC THEORY OF SCROLL COMPRESSOR

Displacement Volume and Build-in Volume Ratio

The major geometric parameters of the scroll are shown in Fig. 1.

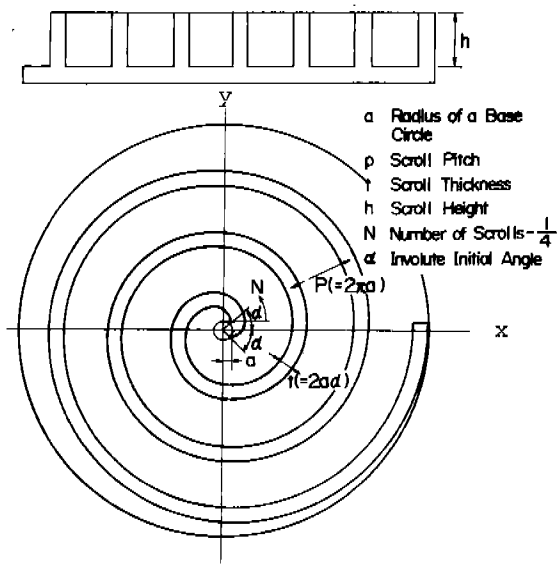

Fig. 1 Scroll Geometric Parameters

The volume of the i-th chamber, $V_i(\theta)$, is obtained from the geometric character of the involute of a circle as follows. (See Fig. 2.)

$$V_i(\theta) = \pi p(p-2t)h \cdot \{(2i-1) - \frac{\theta}{\pi}\} \qquad (1)$$

$$i = 2 \qquad 0 \leq \theta < \theta^*$$

$$3 \leq i \leq N \qquad 0 \leq \theta < 2\pi$$

where θ is the orbiting angle, θ^* is the orbiting angle where the discharge commences, and N is the integer. Angle θ^* is usually determined by the interaction between the involute of a circle and the cutter. See APPENDIX I.

The volume of the innermost chamber is given by

$$V_1(\theta) = \frac{1}{3}a^2h\{(\frac{5}{2}\pi - \alpha - \theta)^3 - (\frac{3}{2}\pi - \alpha - \theta)^3\}$$
$$- 2a^2h\alpha(\frac{3}{2}\pi - \theta)^2 - \frac{2}{3}a^2h\alpha^3 + (-S + 2S') \cdot h$$

Pd Discharge Pressure
Ps Suction Pressure

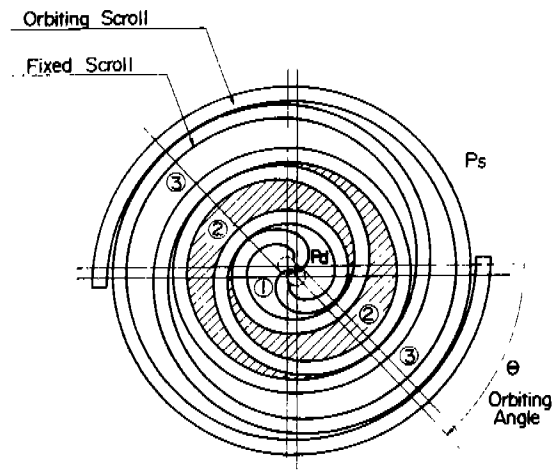

Fig. 2 Compression Chamber of Scroll Compressor

$$0 \leq \theta < \theta^* \qquad (2)$$

$$V_2(\theta) = \frac{1}{3}a^2h\{(\frac{9}{2}\pi - \alpha - \theta)^3 - (\frac{7}{2}\pi - \alpha - \theta)^3\}$$
$$- 2a^2h\alpha(\frac{7}{2}\pi - \theta)^2 - \frac{2}{3}a^2h\alpha^3$$
$$+ (-S + 2S') \cdot h \qquad \theta^* \leq \theta < 2\pi$$

where S is given in APPENDIX II, and S' is the shaded area shown in APPENDIX I. The displacement volume, V_s, is obtained from Eq. (1), where $\theta = 0$.

$$V_s = (2N - 1) \cdot \pi p(p - 2t)h \qquad (3)$$

The nondimensional volume of the compression chamber is shown in Fig. 3 using Eq. (1) and Eq. (2). The pressure is calculated by assuming the isentropic or polytropic processes.

The build-in volume ratio, v, is obtained from Fig. 3 as follows.

$$v = \frac{2N - 1}{3 - \frac{\theta^*}{\pi}} \qquad (4)$$

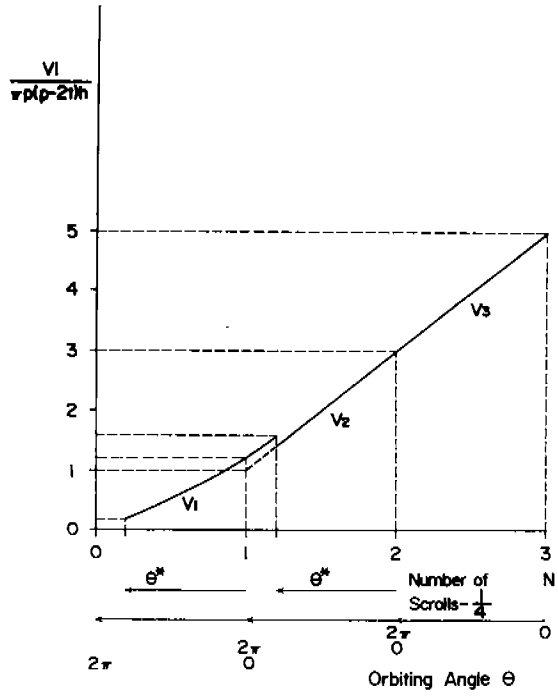

Fig. 3 Displacement Volume

When the rotational speed is constant ($\theta = \omega t$, t; time) the ideal discharge velocity, u, is calculated by the incompressible equation of continuity, i.e., $dV/dt = -u \cdot A_d$, and given as follows;

$$u = (1 - \frac{2\alpha}{\pi}) \frac{p^2 h\omega}{A_d}(1 - \frac{\theta}{2\pi}) \quad 0 \leq \theta < \theta^*$$
$$= (1 - \frac{2\alpha}{\pi}) \frac{p^2 h\omega}{A_d}(2 - \frac{\theta}{2\pi}) \quad \theta^* \leq \theta < 2\pi \qquad (5)$$

where ω is the angular velocity and A_d is the cross sectional area of the discharge port. The nondimensional discharge velocity is shown in Fig. 4.

The mass of the involute of a circle (finite width) m_i is given by

$$m_i \simeq \frac{1}{2} a\beta^2 th \cdot \rho \qquad (6)$$

where $\beta = (2N + \frac{1}{2})\pi$, ρ is the density of the material and the interaction between the cutter and the involute is neglected.

The center of gravity of the involute of a circle (finite width) is given by

$$x_G = 2a(-\cos\beta + 9\frac{\beta}{3\beta^2 + \alpha^2}\sin\beta + 9\frac{\alpha\cos\beta - \sin\alpha}{3\alpha\beta^2 + \alpha^3})$$

$$y_G = 2a(-\sin\beta - 9\frac{\beta}{3\beta^2 + \alpha^2}\cos\beta + \frac{9}{3\beta^2 + \alpha^2}\sin\beta)$$

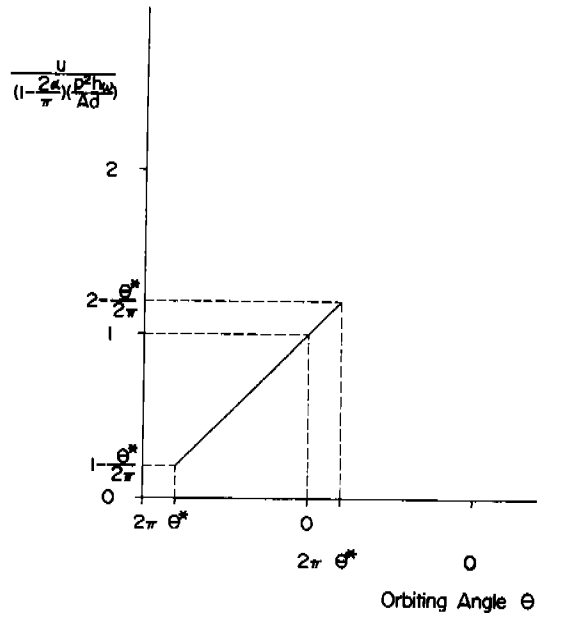

Fig. 4 Discharge Velocity (Ideal)

Pressure Load and Torque

The tangential force, F_θ, is given from the scroll compressor geometry shown in Fig. 2 as follows.

$$F_\theta = P_s ph \sum_{i=1}^{N} (2i - \frac{\theta}{\pi}) \cdot (\rho_i - \rho_{i+1}) \qquad (8)$$

where P_s is the suction pressure and ρ_i is the pressure ratio ($= P_i/P_s = (V_s/V_i)^\kappa$; κ specific heat ratio).

The inward radial force, F_r, is given by

$$F_r = 2P_s ah(\rho_1 - 1) \qquad (9)$$

(The centrifugal force is caused by the orbiting scroll movement. The direction of the force is radially outward.)

The axial force (thrust) is given by

$$F_t = \pi P_s p^2 \{\frac{A}{\pi p^2}(\rho_1 - 1) + \sum_{i=2}^{N} (2i - 1 - \frac{\theta}{\pi}) \cdot (\rho_i - 1)\}$$
$$0 \leq \theta < \theta^* \qquad (10)$$

$$= \pi P_s p^2 \{\frac{A}{\pi p^2}(\rho_1 - 1) + \sum_{i=3}^{N}(2i - 1 - \frac{\theta}{\pi}) \cdot (\rho_i - 1)\} \qquad *\theta \leq \theta < 2\pi$$

The analytical expressions of A in Eq.(10) are given in APPENDIX III.

The torque to compress the gas is given as follows.

$$T = F_\theta \cdot r \tag{11}$$

where r is the crank radius and

$$r = \frac{p}{2} - t$$

When the orbiting scroll shaft center coincides with the center of a base circle of the involute, F_θ works on the center between the base circle of the orbiting scroll and that of the fixed scroll. Therefore a torque appears which tends to rotate the orbiting scroll around its own axis, and the direction of the rotation is the same as that of the drive shaft. The torque, T_s, is given by

$$T_s = T/2 \tag{12}$$

The calculated results of Eqs. (8) ∿ (12) at the build-in pressure ratio are shown in Fig. 5.

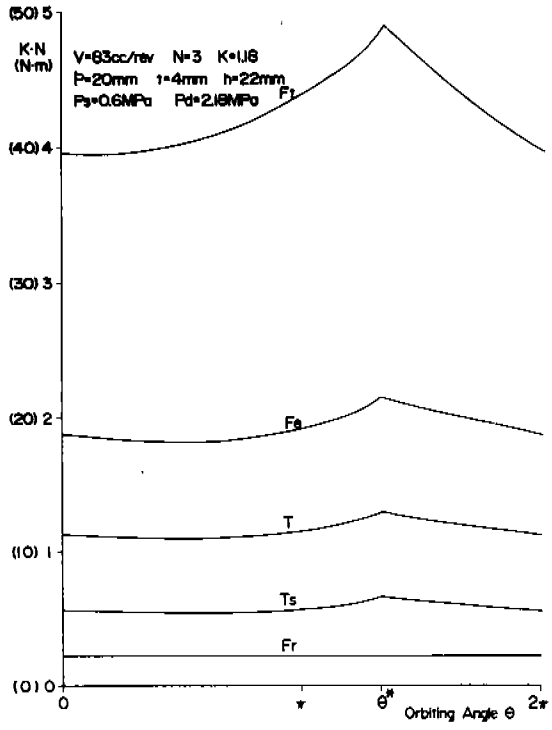

Fig. 5 Force and Torque of Scroll Compressor (Ideal)

EQUATION OF MOTION FOR THE ORBITING SCROLL AND THE OLDHAM COUPLING

Equation of Motion

The forces acting on the orbiting scroll are shown in Fig. 6. The mechanical model in Fig. 6 is for the fixed radius crank. In Fig. 6,

$$F_c = m_s\, r\, (\frac{d\theta}{dt})^2$$

$$F_m = m_s \frac{d^2}{dt^2}(r\theta)$$

The forces acting on the Oldham coupling are shown in Fig. 7.

The equations of motions are given as follows.

Oldham coupling; x-wise balance

$$-\mu_1 F_1 - \mu_2 F_2 + F_3 - F_4 = 0 \tag{13}$$

Oldham coupling; y-wise balance

$$-F_1 + F_2 - \mu_3 F_3 - \mu_4 F_4 - \mu_o m_o g - m_o \frac{d^2}{dt^2}(r\sin\theta) = 0 \tag{14}$$

Oldham coupling; moment balance (See APPENDIX IV)

$$F_1 \cdot n + F_2 \cdot n - F_3 \cdot n - F_4 \cdot n - \mu_1 F_1 \cdot e + \mu_2 F_2 \cdot e + \mu_3 F_3 \cdot e - \mu_4 F_4 \cdot e + \mu_o m_o g \cdot x' = 0 \tag{15}$$

Orbiting scroll; moment balance (See APPENDIX V)

$$F_\theta \frac{r}{2} + (\mu_t F_t \sin\theta \cdot y - \mu_t F_t \cos\theta \cdot x) - F_1 \cdot n - F_2 \cdot n + \mu_1 F_1 \cdot e - \mu_2 F_2 \cdot e + M_B = 0 \tag{16}$$

F_i (i = 1 ∿ 4) is obtained by solving Eqs. (13) ∿ (16) simultaneously and given as follows.

$$F_1 = \frac{1}{E}\{D \cdot F - B \cdot G\}$$

$$F_2 = \frac{1}{E}\{-C \cdot F + A \cdot G\}$$

$$F_3 = \frac{1}{E \cdot E'}\{(C'D - CD') \cdot F + (AD' - BC') \cdot G\} \tag{17}$$

$$F_4 = \frac{1}{E \cdot E''}\{(C''D - CD'') \cdot F + (AD'' - BC'') \cdot G\}$$

(A ∿ F in Eqs. (17) are given in APPENDIX VI.)

When the friction is neglected and the

rotational speed is constant, F_i $(i = 1 \sim 4)$ is calculated as follows.

$$F_1 = \frac{F_\theta \cdot \frac{r}{2}}{2n} + \frac{m_o r\omega^2 \sin\theta}{2}$$

$$F_2 = \frac{F_\theta \cdot \frac{r}{2}}{2n} - \frac{m_o r\omega^2 \sin\theta}{2} \qquad (18)$$

$$F_3 = \frac{F_\theta \cdot \frac{r}{2}}{2n}$$

$$F_4 = \frac{F_\theta \cdot \frac{r}{2}}{2n}$$

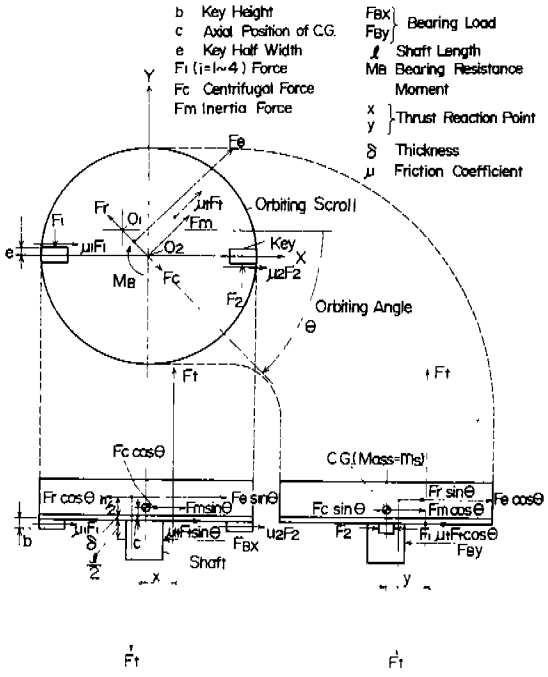

Fig. 6 Orbiting Scroll Motion

Radial Sealing Force

The tangential force, f_θ, and radial force, f_r, on the orbiting scroll bearing are respectively obtained from Fig. 6.

$$f_\theta = F_\theta + F_m + \mu_t F_t + (\mu_1 F_1 + \mu_2 F_2)\sin\theta - (F_1 - F_2)\cos\theta \qquad (19)$$

$$f_r = -F_r + F_c + (\mu_1 F_1 + \mu_2 F_2)\cos\theta + (F_1 - F_2)\sin\theta \qquad (20)$$

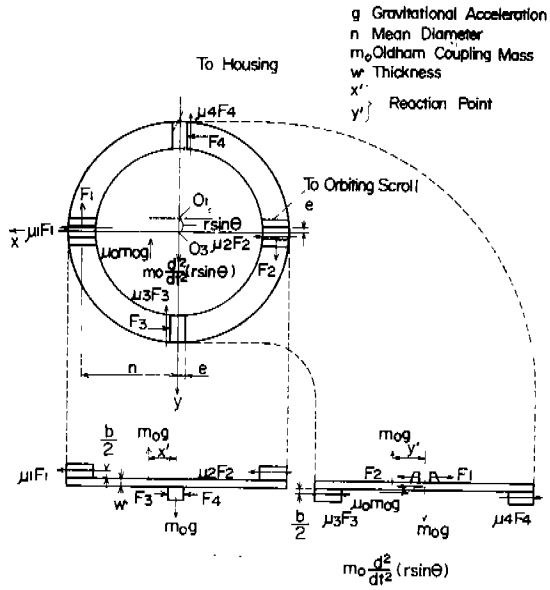

Fig. 7 Oldham Coupling Motion

The radial sealing force, f_s, is given as follows, when the compliant crank mechanism[5),6)] is employed as shown in Fig. 8.

$$f_s = f_r - f_\theta \cdot \tan\theta_p \qquad (21)$$

where θ_p is the offset angle. When there is no friction and the rotational speed is constant

$$f_s = F_c - F_r + m_o r\omega^2 \sin^2\theta - (F_\theta - m_o r\omega^2 \sin\theta\cos\theta)\cdot\tan\theta_p \qquad (22)$$

where m_o is the mass of the Oldham coupling.

The influence of the Oldham coupling in Eq. (22) is proportional to the mass of the Oldham coupling and the square of the rotational speed. The effect of the Oldham coupling on the radial sealing force changes twice as fast as the rotational speed.

The calculated F_i $(i = 1 \sim 4)$ is shown in Fig. 9, and the radial sealing force, f_s, is shown in Fig. 10, where θ_p is the parameter. In Fig. 9 and 10, the friction coefficients shown in Fig. 6 and 7 are included and assumed to be 0.01. The other conditions are shown in APPENDIX VII. (The tangential, radial and axial forces and torque are also obtainable when

there is friction.)

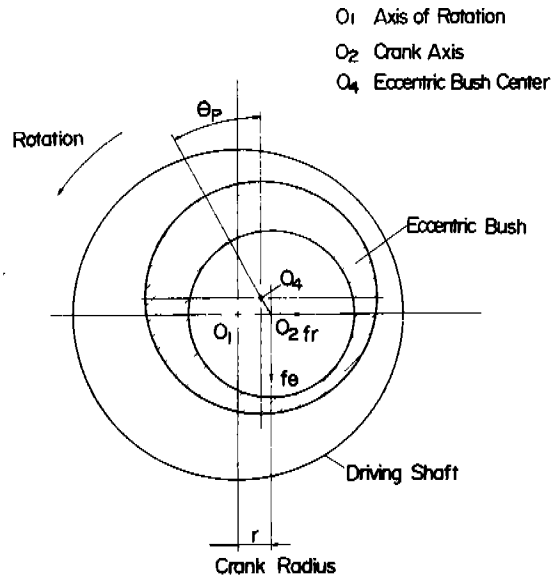

Fig. 8 Radial Sealing Mechanism

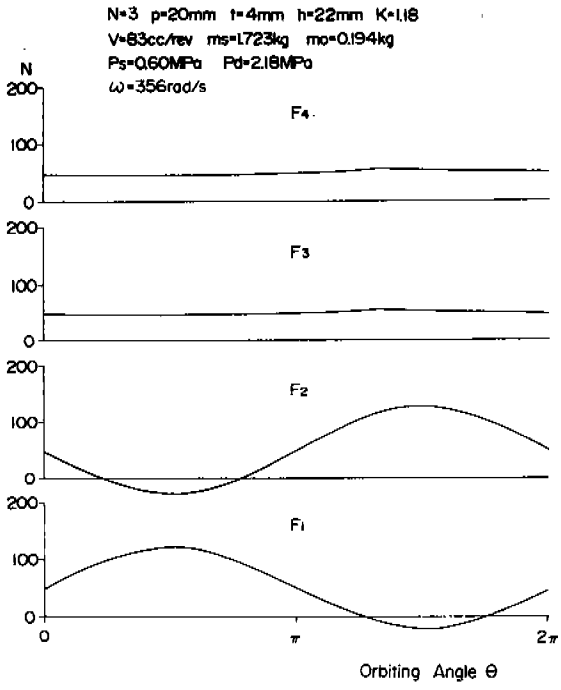

Fig. 9 Oldham Coupling Contact Force Fi(i = 1 ∿ 4) (with Friction)

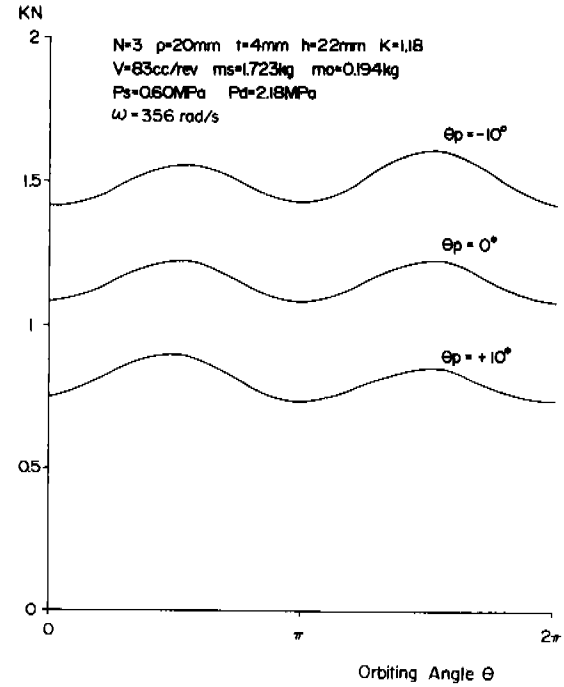

Fig. 10 Radial Sealing Force (with Friction)

Overturning Moment and Stability of Orbiting Scroll

The overturning moment occurs on the orbiting scroll primarily because the radial bearing supports the orbiting scroll in a different plane from that where the radial and tangential forces occur. This overturning moment for the fixed radius crank is given from Fig. 6 by

$$M = \sqrt{M_x^2 + M_y^2} \tag{23}$$

where

$M_x = F_t(y - r\sin\theta)$ moment around x-axis

$M_y = F_t(x + r\cos\theta)$ moment around y-axis

and x and y are given in APPENDIX V.

The thrust reaction point measured from the axis of rotation, r_m, is equal to $\sqrt{(x + r\cos\theta)^2 + (y - r\sin\theta)^2}$ and the non-dimensional ratio, ε,[11] to the thrust bearing substantial outer radius, r_t, is given by

$$\varepsilon = \frac{r_m}{r_t} = \frac{M}{F_t \cdot r_t} \tag{24}$$

To realize the stable operation of the orbiting scroll, it is necessary that

$$\varepsilon < 1 \qquad (25)$$

To enhance the axial sealing, the back pressure may be applied to the orbiting scroll.[3] However, the stability condition of Eq. (25) can be violated when the compressor starts and the back pressure changes rapidly. Therefore the back pressure methods is not suitable for the variable pressure ratio operation.

The calculated overturning moment is shown in Fig. 11. ε is shown in Fig. 12. The conditions for the calculation are the same as those of Fig. 9 and 10. See APPENDIX VII. (When the compliant crank mechanism is employed, the radial sealing force is supported by the fixed scroll. Therefore the overturning moment which acts on the thrust bearing is reduced.)

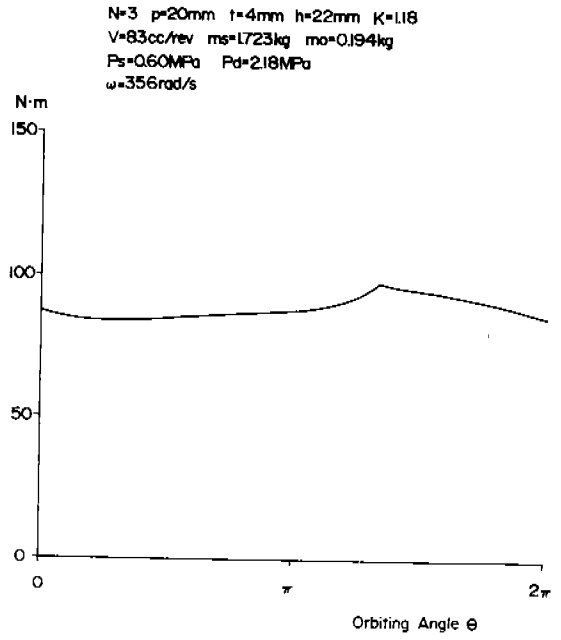

Fig. 11 Overturning Moment (with Friction)

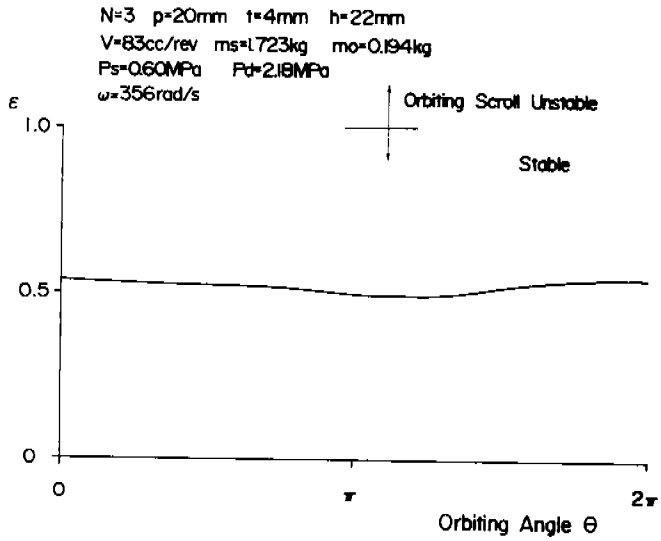

Fig. 12 Orbiting Scroll Stability (with Friction)

CONCLUSION

The analytical model is established for the scroll machine which employs the involute of a circle.

(1) The geometric parameters of the scroll compressor are shown. The center of gravity and the mass can be calculated for the finite width involute of a circle.

(2) The displacement volume is given and the pressure ratio is estimated by assuming the isentropic or polytropic processes. The tangential, radial and axial forces are calculated.

(3) The equations of motion, including the friction, are established for the orbiting scroll and the Oldham coupling. The effect of the Oldham coupling motion on the orbiting scroll is clarified. The radial sealing force is influenced by the Oldham coupling inertia force, which is proportional to the mass of the Oldham coupling and the square of the rotational speed. The effect of the Oldham coupling on the orbiting scroll changes twice as fast as the rotational frequency.

(4) The overturning moment is estimated and the stability condition for the orbiting scroll is clarified.

APPENDIX I

When the involute of a circle is created by a cutter with outer diameter p - t, the innermost shaded area in Fig. A1 is cut away by the interaction between the cutter and the involute. The discharge angle, θ^*, is determined by point P. The curve between P and Q is a circle with the same radius as that of the cutter, and the

dotted curve between P and Q is the involute of a circle in Fig. A1.

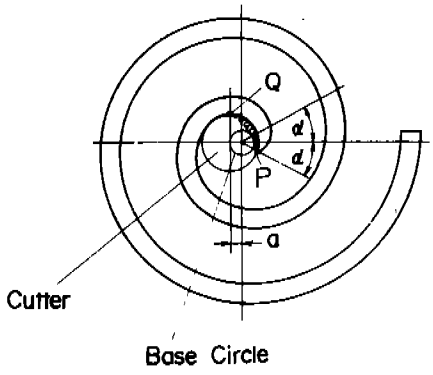

Fig. A1 Interaction Between Cutter and Involute

APPENDIX II

S in Eq. (2) is given by the shaded area in Fig. A2.

APPENDIX III

In Eq. (10),

$$A = \frac{1}{3}a^2\{(\frac{5}{2}\pi - \theta)^3 - (\frac{3}{2}\pi - \theta)^3\} - S \qquad 0 \le \theta < \theta^*$$

$$= \frac{1}{3}a^2\{(\frac{9}{2}\pi - \theta)^3 - (\frac{7}{2}\pi - \theta)^3\} - S \qquad \theta^* \le \theta < 2\pi$$

where S is given in Fig. A2.

APPENDIX IV

In Eq. (15), x' is obtained from the moment balance of the Oldham coupling around the sliding surface. In Fig. 7, y' is also obtained from the moment balance.

$$x' = \frac{(\mu_1 F_1 + \mu_2 F_2)(b + w)}{m_o g}$$

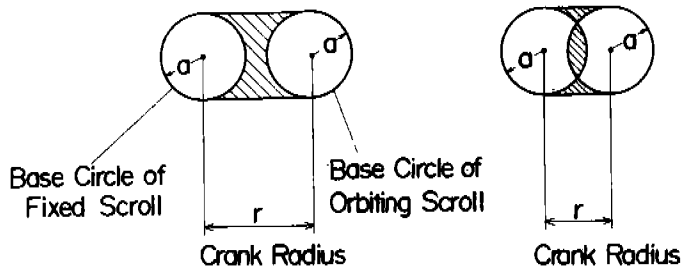

Fig. A2 Area Between Base Circles

$$y' = \frac{-F_1 + F_2}{m_o g}(\frac{b}{2} + \frac{w}{2}) + \frac{\mu_3 F_3 + \mu_4 F_4}{m_o g}(\frac{b}{2} + \frac{w}{2}) + \mu_o \frac{w}{2}$$

APPENDIX V

In Eq. (16), x and y are obtained from the moment balance around the thrust bearing surface. From Fig. 6, x and y are given as follows.

$$x = \{\frac{F_c}{F_t}(\frac{\ell}{2} + c) - \frac{F_r}{F_t}(\frac{h}{2} + \delta + \frac{\ell}{2}) - \frac{r}{2}\}\cos\theta + \{\frac{F_\theta}{F_t}(\frac{h}{2} + \delta + \frac{\ell}{2}) + \frac{\ell}{2}\mu_t + \frac{F_m}{F_t}(\frac{\ell}{2} + c)\}\sin\theta + \frac{\mu_1 F_1 + \mu_2 F_2}{F_t}(\frac{\ell}{2} - \frac{b}{2})$$

$$y = \{\frac{F_\theta}{F_t}(\frac{h}{2} + \delta + \frac{\ell}{2}) + \frac{\ell}{2}\mu_t + \frac{F_m}{F_t}(\frac{\ell}{2} + c)\}\cos\theta + \{-\frac{F_c}{F_t}(\frac{\ell}{2} + c) + \frac{F_r}{F_t}(\frac{h}{2} + \delta + \frac{\ell}{2}) + \frac{r}{2}\}\sin\theta + \frac{F_2 - F_1}{F_t}(\frac{\ell}{2} - \frac{b}{2})$$

APPENDIX VI

In Eqs. (17), A ∿ F are given as follows.

$$A = (n - e\mu_1) + \mu_1\mu_t(\frac{\ell}{2} - \frac{b}{2})\cos\theta + \mu_t(\frac{\ell}{2} - \frac{b}{2})\sin\theta$$

$$B = (n + e\mu_2) + \mu_2\mu_t(\frac{\ell}{2} - \frac{b}{2})\cos\theta - \mu_t(\frac{\ell}{2} - \frac{b}{2})\sin\theta$$

$$C = (\mu_1\mu_4 - 1)\{(n - e\mu_3) + (n + e\mu_4)\} - (\mu_3 + \mu_4)\{\mu_1(n + e\mu_4) + (n - e\mu_1) + \mu_o\mu_1(b + w)\}$$

$$D = (\mu_2\mu_4 + 1)\{(n - e\mu_3) + (n + e\mu_4)\} - (\mu_3 + \mu_4)\{\mu_2(n + e\mu_4) + (n + e\mu_2) + \mu_o\mu_2(b + w)\}$$

$$C' = \mu_1(n + e\mu_4) + (n - e\mu_1) + \mu_o\mu_1(b + w)$$

$$D' = \mu_2(n + e\mu_4) + (n + e\mu_2) + \mu_o\mu_2(b + w)$$

$$C'' = -\mu_1(n - e\mu_3) + (n - e\mu_1) + \mu_o\mu_1(b + w)$$

$$D'' = -\mu_2(n - e\mu_3) + (n + e\mu_2) + \mu_o\mu_2(b + w)$$

$$E = A \cdot D - B \cdot C$$

$$E' = (n - e\mu_3) + (n + e\mu_4)$$

$$F = F_\theta\frac{r}{2} + M_B + \mu_t\{F_r(\frac{h}{2} + \delta + \frac{\ell}{2}) - F_c(c + \frac{\ell}{2}) + F_t\frac{r}{2}\}$$

$$G = E'\{\mu_o m_o g + m_o\frac{d^2}{dt^2}(r\sin\theta)\}$$

The friction coefficients of the sliding surface are given as follows.

Oldham coupling

$$\mu_1 = |\mu_1| \cdot \sin\theta/|\sin\theta|$$

$$\mu_2 = |\mu_2| \cdot \sin\theta/|\sin\theta|$$

$$\mu_3 = |\mu_3| \cdot \cos\theta/|\cos\theta|$$

$$\mu_4 = |\mu_4| \cdot \cos\theta/|\cos\theta|$$

$$\mu_o = |\mu_o| \cdot \cos\theta/|\cos\theta|$$

Thrust bearing

$$\mu_t$$

APPENDIX VII

In Fig. 9, 10, 11 and 12, the other parameters for the calculation are given as follows.

$c = 7.13$ mm

$\ell = 38$ mm

$\delta = 11$ mm

$n = 60$ mm

$e = 3$ mm

$b = 8$ mm

$w = 4.2$ mm

$r_t = 40$ mm

REFERENCES

[1] Creux, L., "Rotary Engine", US.P. 801,182, 1905.

[2] Hiraga, M., "The Spiral Compressor. An Innovative Air Conditioning Compressor for the New Generation Automobiles", 1983 SAE Paper, No. 830540.

[3] Arai, N. et al., "Scroll Compressor and Its Application to Packaged Air Conditioner (in Japanese)", The Hitachi Hyoron, Vol. 65, No. 6, June 1983, pp.31-36.

[4] Morishita, E. et al., "Scroll Compressor (in Japanese)", Mitsubishi-Denki Giho, Vol.58, No.5, May 1984

[5] Ekelöf, J., "Rotary Pump or Compressor", US.P. 1,906,142 Apr. 25, 1933.

[6] Compagnie pour la Fabrication des Compteurs et Matériel d'Usines à Gaz, "Improvements in Apparatus for Fluids such as Engine, Pumps, Compressors, Meters and the Like, Comprosing a Member Operated by an Orbitary Movement", U.K. Patent Specification 486,192 May 31, 1938.

[7] Bennett, J.S., "Rotary Fluid Pump or Motor with Intermeshed Spiral Walls", US.P. 3,817,664, June 18, 1974.

[8] McCullough, J.E., "Positive Fluid Displacement Apparatus", US. P. 3,924,977, Dec. 9, 1975.

[9] Moore, R.W., Jr. et al., "A Scroll Compressor for Shipboard Helium Liquefier Systems", Purdue Compressor Technology Conference, July 1976, pp.417-422.

[10] McCullough, J.E. and Hirschfeld, F., "The Scroll Machine - An Old Principle with a New Twist", Mechanical Engineering, Dec. 1979, pp.46-51.

[11] Rumbarger, J.H., "Thrust Bearings with Eccentric Loads", Machine Design, Feb. 15, 1962, pp.172-179.